Aminobacter sp. MSH1 mineralises the groundwater micropollutant 2,6-dichlorobenzamide through a unique chlorobenzoate catabolic pathway

Bart Raes[1], Benjamin Horemans[1], Daniel Rentsch[2], Jeroen T'Syen[1], Maarten G. K. Ghequire[3], René De Mot[3], Ruddy Wattiez[4], Hans-Peter E. Kohler[5], Dirk Springael[1]*

[1] Division of Soil and Water management, Department of Earth and Environmental Sciences, Faculty of Bioscience Engineering, KU Leuven, Leuven, Belgium

[2] Laboratory for Functional Polymers, Empa, Swiss Federal Laboratories for Materials Science and Technology, Dübendorf, Switzerland

[3] Centre of Microbial and Plant Genetics, KU Leuven, Leuven, Belgium

[4] Department of Proteomics and Microbiology, University of Mons, Mons, Belgium

[5] Department of Environmental microbiology, Eawag, Swiss Federal Institute of Aquatic Science and Technology, Dübendorf, Switzerland

* Corresponding author: Division of Soil and Water management, Department of Earth and Environmental Sciences, Faculty of Bioscience Engineering, Kasteelpark Arenberg 20, KU Leuven, Leuven, Belgium; Tel. 32 16 32 16 04;
Fax 32 16 32 19 97; e-mail: dirk.springael@kuleuven.be

Keywords
2,6-dichlorobenzamide biodegradation, chlorobenzoate catabolic pathway, bioremediation, drinking water treatment

Abstract

2,6-dichlorobenzamide (BAM) is a major groundwater micropollutant posing problems for drinking water treatment plants (DWTPs) that depend on groundwater intake. *Aminobacter* sp. MSH1 uses BAM as a sole source of carbon, nitrogen and energy and is considered a prime biocatalyst for groundwater bioremediation in DWTPs. Its use in bioremediation requires knowledge on its BAM-catabolic pathway which is currently restricted to the amidase BbdA converting BAM into 2,6-dichlorobenzoic acid (2,6-DCBA) and the mono-oxygenase BbdD transforming 2,6-DCBA in 2,6-dichloro-3-hydroxybenzoic acid. Here, we show that the 2,6-DCBA catabolic pathway is unique and differs substantially from catabolism of other chlorobenzoates. BbdD catalyses a second hydroxylation forming 2,6-dichloro-3,5-dihydroxybenzoic acid. Subsequently, glutathione-dependent dehalogenases (BbdI and BbdE) catalyse the thiolytic removal of a first chlorine. The remaining chlorine is then removed hydrolytically by a dehalogenase of the α/β hydrolase superfamily (BbdC). BbdC is the first enzyme in that superfamily associated with dehalogenation of chlorinated aromatics and appears to represent a new subtype within the α/β hydrolase dehalogenases. The activity of BbdC yields a unique trihydroxylated aromatic intermediate for ring cleavage that is performed by an extradiol dioxygenase (BbdF) producing 2,4,6-trioxoheptanedioic acid which is likely converted to Krebs cycle intermediates by BbdG.

Introduction

2,6-dichlorobenzamide (BAM) is a transformation product of the widely used herbicide dichlobenil [1] and is a major groundwater micropollutant in Europe often detected above the EU threshold for drinking water of 0.1 µg.L^{-1} [2–4]. In Europe, groundwater is an important drinking water resource and BAM contamination results in either costly closure of extraction wells or the inclusion of expensive remediation modules such as activated carbon filtration in drinking water treatment plants (DWTPs) [5]. Bioremediation of BAM-contaminated groundwater was suggested as an environmentally friendly and cost-effective alternative treatment method in DWTPs [1,6]. *Aminobacter sp.* MSH1 has the unusual ability to mineralise BAM and to use it as a sole source of carbon, nitrogen and energy [7,8]. MSH1 survives well under oligotrophic conditions encountered

in DWTPs [9], develops biofilms [10], and mineralises BAM at trace concentrations [8]. The strain is considered a prime biocatalyst for treating BAM-contaminated groundwater in DWTPs by bioaugmentation of dedicated filtration modules [1]. Promising results were obtained in both laboratory and pilot-scale studies with bioaugmented sand filters, showing BAM removal below the EU threshold for five to six weeks [11,12]. To further improve our understanding of growth-linked BAM degradation at micropollutant concentrations (ng L^{-1} - µgL^{-1} range) by strain MSH1, it is crucial to identify the underlying biochemical processes. Moreover, such knowledge will support the strains' application in DWTPs for instance through aiding in process monitoring. We previously reported that the BAM-catabolic pathway in MSH1 is encoded on two plasmids, i.e., pBAM1 and pBAM2. pBAM1 carries the *bbdA* gene encoding the amidase BbdA that converts BAM into 2,6-dichlorobenzoic acid (2,6-DCBA) [13], a chlorobenzoate isomer for which no catabolic pathway has been described yet. pBAM2 harbours two gene clusters (i.e. *bbdR1B1B2B3CDE* and *bbdR2FGHIJ*) that are likely involved in the conversion of 2,6-DCBA to Krebs cycle intermediates [14]. Within the *bbdR1B1B2B3CDE* gene cluster, *bbdD* encodes a monooxygenase that converts 2,6-DCBA into 2,6-dichloro-3-hydroxybenzoic acid (2,6-diCl-3-OHBA) [14]. However, the further degradation steps are currently unknown. In this study, we explored the BAM/2,6-DCBA catabolic pathway in strain MSH1 beyond 2,6-diCl-3-OHBA. We identified the responsible enzymes and the pathway intermediates involved.

Materials and methods

Strains, cultivation conditions and chemicals. Wild type *Aminobacter* sp. MSH1 (MSH1 wt) was grown in mineral salts (MS) medium containing 1 mM BAM at 25°C [15]. *Aminobacter* sp. M6.100g, a variant of MSH1 lacking pBAM2 and unable to degrade 2,6-DCBA [14], was grown on R2B [16]. Strain M6.100g variants carrying pRU1097 derivatives containing one of the pBAM2 catabolic genes *bbdC, bbdD, bbdE, bbdF, bbdI or* $bbdJ_4$ under the control of the *bbdA* constitutive promoter (referred to as $M6_{bbdC}$, $M6_{bbdD}$, $M6_{bbdE}$, $M6_{bbdF}$, $M6_{bbdI}$, $M6_{bbdJ4}$,respectively) or carrying the pRU1097 vector without insert (referred to as $M6_{pRU}$) were reported elsewhere and were grown on R2B supplemented with 10 mg L^{-1} gentamycin [14]. BAM, 2,6-DCBA, 3,5-dihydroxybenzoic acid (3,5-diOHBA) and chelidonic acid were purchased from Sigma-Aldrich (Belgium), 2,6-dichloro-3-

hydroxybenzoic acid (2,6-diCl-3-OHBA) from SynphaBase AG (Switzerland), 2,6-dichloro-3,5-dihydroxybenzoic acid (2,6-diCl-3,5-diOHBA), 2-chloro-3,5-dihydroxybenzoic acid (2-Cl-3,5-diOHBA) from Carbosynth (United Kingdom) and 2,3,5-trihydroxybenzoic acid (2,3,5-triOHBA) from Akos Consulting & Solutions GmbH (Germany). Ellman's reagent was purchased from ThermoFisher Scientific (USA), NADPH from Carl Roth GmbH (Germany). Reduced glutathione (GSH) and oxidized glutathione (GSSG) were acquired from J&K Scientific GmbH (Germany).

Degradation of 2,6-diCl-3-OHBA by MSH1 wt. MSH1 wt was grown as a 200 mL culture as described above. When all BAM was degraded, the culture was centrifuged (6000 *x g*, 15 min, 18°C), washed three times with 10 mM $MgSO_4$, resuspended in 25 mL MS medium containing 0.9 mM 2,6-diCl-3-OHBA and incubated at 25°C. At regular intervals, 200 µL samples were taken, acidified with 2 µL of 37 % HCl and centrifuged (21380 *x g*, 5 min). 170 µL of the supernatant was used to assess 2,6-diCl-3-OHBA conversion and detection of new pathway intermediates by reverse phase ultrahigh performance liquid chromatography (RP-UHPLC). Tests were done in triplicate.

Degradation of 2,6-DCBA or 2,6-diCl-3-OHBA by M6$_{bbdD}$ cells. M6$_{bbdD}$ was grown in a 200 mL culture as described above and harvested at an optical density at 600 nm (OD_{600nm}) of 0.9. After centrifugation (6000 *x g*, 15 min, 18°C), the pellet was washed three times with 10 mM $MgSO_4$, resuspended in 25 mL MS medium containing 1 mM of 2,6-DCBA or 2,6-diCl-3-OHBA and incubated at 25°C with or without 1 mM NADH. At regular time intervals, 200 µL samples were taken and processed as described above to assess 2,6-DCBA conversion and product formation using RP-UHPLC. Cells of M6$_{pRU}$ were used as a negative control and tests were done in triplicate.

Preparation of crude protein extracts. M6$_{bbdC}$, M6$_{bbdD}$, M6$_{bbdE}$, M6$_{bbdF}$, M6$_{bbdI}$, M6$_{bbdJ4}$, and M6$_{pRU}$ were grown in 200 mL cultures as described above. At an OD_{600nm} of 0.9, cultures were harvested by centrifugation (6000 *x g*, 15 min, 4°C) and washed with 10 mM $MgSO_4$. The pellets were frozen at -20°C for one hour, thawed on ice and resuspended in 5 mL pre-cooled lysis buffer (4°C, 50 mM Tris-HCl, 100 mM NaCl, 5 % (V/V) glycerol at pH 7.5). The suspensions were sonicated on ice for 10 min with a 30 s pulse, 30 s pause and a 40 % amplitude (Vibra-Cell™ VCX 130, Sonics, USA). Two µL of Benzonase® nuclease (25 KU, Sigma-Aldrich) was added and the mixtures were incubated for 10 min at 25°C. After centrifugation (21380 *x g*, 15 min, 4°C), the supernatants were

filtered through a 0.2 µm filter (Fisherbrand) and stored at 4°C. Total protein concentrations were determined with the Qubit 3.0 fluorometer (Invitrogen), according to the manufacturers protocol and adjusted to a total protein concentration of approximately 2500 ng/µL. Recombinant protein expression was verified with sodium dodecyl sulphate polyacrylamide gel electrophoresis (SDS-PAGE) as described in the supporting information (p. S3). Results of the SDS-PAGE are shown in Figure S1.

Isolation and identification of BbdC by anion exchange (AEC) and hydrophobic interactions chromatography (HIC). The detailed procedure to isolate BbdC from a crude extract of a MSH1 wt culture is described in the supporting information (p. S4). In short, a crude protein extract of MSH1 wt grown in 1 L MS medium supplemented with 5 mM BAM at 25°C, was prepared as described above except that 20 mL lysis buffer was used. The extract was dialysed and subjected to AEC. Proteins were collected in 2 mL fractions and checked for conversion of 2-Cl-3,5-diOHBA by RP-UHPLC. Active fractions were pooled and subjected to HIC after adding ammonium sulphate. Protein fractions were again tested for activity towards 2-Cl-3,5-diOHBA and analysed with SDS-PAGE, to check protein purity. Proteins in active fractions were identified by LC-MS/MS as described by Breugelmans *et al.* [17].

Enzyme assays. The crude protein extract of M6$_{bbdD}$ was tested by addition of 0.1 volumes to MS medium with 1 mM NADH and 0.5 mM of either 2,6-DCBA or 2,6-diCl-3-OHBA. Crude protein extracts of M6$_{bbdE}$ and M6$_{bbdI}$ were tested by addition of 0.1 volumes to MS medium containing 1 mM GSH and 0.5 mM of either 2,6-DCBA, 2,6-diCl-3-OHBA, 2,6-diCl-3,5-diOHBA or 2-Cl-3,5-diOHBA. The M6$_{bbdC}$ protein extract was tested by adding 0.1 volumes to MS medium containing either 0.5 mM 2,6-diCl-3-OHBA, 2,6-diCl-3,5-diOHBA or 2-Cl-3,5-diOHBA. To test the activity of M6$_{bbdC}$ under anaerobic conditions, a serum bottle containing MS medium amended with 0.5 mM 2-Cl-3,5-diOHBA and 0.002 mM resazurin as an oxygen indicator, was closed gas-tight with crimp seals and the medium made anaerobic by flushing with N_2 overnight. The M6$_{bbdC}$ protein extract was tested by adding 0.1 volumes to the anaerobic medium. Anaerobic conditions were ensured by performing the assay in an anaerobic chamber (Coy Laboratory Products, USA). The activity of M6$_{bbdF}$ towards 2,3,5-triOHBA was tested by adding 0.1 volumes of extract to MS medium containing 2,3,5-triOHBA. In all assays, 200 µL samples were taken at regular time intervals,

acidified with 2 µL of 37 % HCl, centrifuged (21380 *x g*, 5 min) and analysed for substrate conversion by RP-UHPLC. Activity of $BbdJ_4$ was tested by spectrophotometrically determining the conversion of GSSG to GSH by reaction of GSH with Ellman's reagent [18]. Protein extracts of $M6_{bbdJ4}$ and $M6_{pRU}$ were diluted 20-fold in lysis buffer (50 mM Tris-HCl, 100 mM NaCl, 5 % (v/v) glycerol at pH 7.5) and added as 0.1 volumes to PBS containing either 1 mM GSSG and 1 mM NADPH, 1 mM GSSG or 1 mM NADPH. After one hour, 250 µL samples were added to a reaction mixture consisting of 2.5 mL sodium phosphate buffer (0.1 M, 1 mM EDTA, pH 8.0) and 0.05 mL of 4 mg mL^{-1} Ellman's reagent solution. Samples were incubated for 15 min at 25 °C and absorption at 412 nm was measured with a PerkinElmer UV/Vis Lambda 25 Spectrometer (PerkinElmer, USA). To calculate GSSG conversion rates, absorption was converted into GSH concentrations by means of a standard curve of different GSH concentrations treated with the Ellman's reagent solution and considering the stoichiometric conversion of one GSSG molecule in two GSH molecules. Non-specific absorption was determined with the $M6_{pRU}$ crude extract control and subtracted prior to conversion to GSH concentrations. In all assays, an extract of $M6_{pRU}$ was tested as a negative control and duplicate reactions were performed.

RP-UHPLC analysis. Substrate conversion and product formation was measured by injecting 10 µL samples on a Nexera apparatus (Shimadzu Corp) equipped with a Triart C18 column (150 x 3 mm, 3 µm; YMC) kept at 40°C. Isocratic flow (0.4 mL min^{-1}) of 12 % acetonitrile and 88 % ultrapure water acidified with 0.1 % formic acid was applied and a UV-vis spectrometer at 210 nm was used for detection.

Identification of pathway intermediates. To identify unknown pathway intermediates, liquid chromatography tandem mass spectrometry (LC-MS/MS) or gas chromatography-mass spectrometry (GC-MS) was used. Preparation of metabolites for UHPLC-MS/MS and GC-MS analysis is explained in the supporting information (p. S5). For LC-MS/MS analysis, a LC-MS8045 triple quadrupole mass spectrometer (Shimadzu Corp) coupled to the Nexera UHPLC apparatus was used. The interface, desolvation line and heat block temperatures were kept at 300°C, 250°C and 400°C, respectively. Nebulizing gas flow was set at 3.0 L min^{-1} while drying and heating gas flow rates were 10 L min^{-1}. Ten µL samples were injected and full MS scans and MS^2 scans for all compounds were conducted in the negative ionization mode. For GC-MS analysis, one µl of an *O*-

Bis(trimethylsilyl)trifluoroacetamide (BSTFA) treated sample was injected into a Thermo Scientific Trace GC Ultra equipped with a Zebron ZB % MS column (length 30 m, inner diameter 0.25 mm, film thickness 0.25 µm) and coupled to a Thermo Scientific ITQ 900 Ion Trap mass spectrometer. The temperature program was 7 min at 80°C, followed by an increase of 14°C min^{-1} to 325°C (held for 5 min). The molecular structure of suspected metabolites was further analysed by nuclear magnetic resonance (NMR). Preparation of the metabolites for NMR is explained in the supporting information (p. S5). ^{1}H and ^{13}C NMR data were recorded at 400.1 and 100.6 MHz at 298 K on a Bruker Avance III 400 NMR spectrometer (Bruker Biospin AG, Fällanden, Switzerland). The 1D ^{1}H and ^{13}C NMR spectra, as well as the 2D-correlated ^{1}H-^{13}C HSQC and ^{1}H-^{13}C HMBC NMR experiments were performed using the Bruker standard pulse programs and parameter sets on a 5 mm CryoProbe™ Prodigy probe equipped with z-gradient applying 90° pulse lengths of 11.4 µs (^{1}H) and 10.0 µs (^{13}C). When only limited amounts of material were available (≤ 1 mg of a mixture of metabolites), methanol or DMSO susceptibility-matched Shigemi tubes with about 240 µL of the respective solution were used. The ^{1}H and ^{13}C NMR chemical shifts (δ) in ppm were calibrated to the resonances of methanol at δ = 3.31 / 49.0 or DMSO at 2.49/39.5 ppm for ^{1}H / ^{13}C, respectively.

Results

Identification of 2,6-diCl-3-OHBA degradation products. MSH1 wt cells were incubated with 2,6-diCl-3-OHBA to identify pathway intermediates beyond 2,6-diCl-3-OHBA. 2,6-diCl-3-OHBA was degraded concomitant with the appearance of one larger peak and two smaller peaks in the RP-UHPLC chromatogram, suggesting the formation of three degradation products (referred to as compounds A (larger peak), B and C) (Figure S2). Upon complete depletion of 2,6-diCl-3-OHBA, the peak height of compound A decreased and finally all compounds disappeared. M6.100g which lacks pBAM2 did not degrade 2,6-diCl-3-OHBA, neither were compounds A, B or C detected. Compounds A, B and C were analysed by LC-MS/MS and NMR from MSH1 wt samples showing around 80 % conversion of 2,6-diCl-3-OHBA. The LC-MS/MS spectrum of compound A showed that the base peak of the $[M-H]^-$ ion had a *m/z* of 220.94 (Table S1). Likely, it contained two chlorine atoms as indicated by the *m/z* 222.94 and *m/z* 224.94 isotopic peaks with relative abundances of 62 % and 10 %, respectively. This suggests that compound A has the molecular

formula $C_7H_4Cl_2O_4$. Its ^1H NMR spectrum (Figure 1A, Table S2) showed a singlet signal at 6.51 ppm which correlates to a carbon at 104.3 ppm in the ^1H-^{13}C HSQC spectrum (Figure 1C) and to two quaternary carbons at 154.0 ppm and 108.6 ppm in the ^1H-^{13}C HMBC spectrum (Figure 1D). Moreover, only five distinct signals were observed in the ^{13}C NMR spectrum (Figure 1B, Table S3, carbon atom numbering for all compounds analysed by NMR is shown in Figure S3), indicating that the compound is symmetrical. From the molecular formula, only two symmetric benzoic acid derivatives could be envisioned, i.e., 2,6-diCl-3,5-diOHBA and 3,5-diCl-2,6-diOHBA. Consequently, compound A was identified as 2,6-diCl-3,5-diOHBA since 2,6-diCl-3-OHBA was the substrate. The base peak of the $[M-H]^-$ ion of compound B had a *m/*z of 186.98 (Table S1). A secondary isotopic peak at *m/*z 188.98 with a relative abundance of 32 % suggests the presence of one chlorine atom, indicating that the molecular formula of compound B is $C_7H_5ClO_4$. In the ^1H NMR spectrum two signals at 6.45 ppm (*d*, J = 2.8 Hz) and 6.48 ppm (*d*, J = 2.8 Hz) were present, indicating two protons *meta* positioned to each other on the aromatic moiety (Figure 1E, Table S2). A 1D ^{13}C NMR spectrum could not be obtained due to the low amount of compound B in the sample (< 0.05 mg). The ^1H-^{13}C HSQC correlations showed that the two protons are bound to carbons at 104.9 ppm and 107.2 ppm, respectively (Figure 1F, Table S2). From the ^1H-^{13}C HMBC correlation (Figure 1G) of the proton at 6.45 ppm to the carboxylic acid group at 168.1 ppm, it is clear that this proton must be in *ortho* to the carboxyl group. Subsequently, all remaining carbon atoms were assigned and compound B was identified as 2-Cl-3,5-diOHBA. Similar to compound A, the $[M-H]^-$ ion base peak of compound C had a *m/*z of 220.94 with two isotopic peaks of *m/*z 222.94 and *m/*z 224.94 and relative abundances of 62 % and 10 %, respectively. This suggests the presence of two chlorine atoms (Table S1) and a molecular formula of $C_7H_4Cl_2O_4$. In contrast to compound A, seven distinct signals were observed by ^{13}C NMR (Figure 1I, Table S3), suggesting that compound C is non-symmetrical. Only one singlet signal at 6.74 ppm was observed in the ^1H NMR spectrum (Figure 1H, Table S2). Under the assumption that no switch in positions of chlorine atoms occurred and that they both are still in *ortho* position to the carboxyl group, compound C must be 2,6-diCl-3,4-diOHBA. The analysis of the ^1H, HSQC and HMBC NMR data (Figure 1H, J, K, Tables S2, S3) supported this assumption. Confirmation of the structures of compounds A and B was obtained by comparing the LC-MS/MS and NMR spectra to those obtained from authentic 2,6-

diCl-3,5-diOHBA and 2-Cl-3,5-diOHBA (Figure S4, Tables S2, S3). Authentic 2,6-diCl-3,4-diOHBA was not available. MSH1 wt degraded and grew on authentic 2,6-diCl-3,5-diOHBA and 2-Cl-3,5-diOHBA while M6.100g, lacking pBAM2, did not (data not shown).

Conversion of 2,6-DCBA into 2,6-diCl-3,5-diOHBA is catalysed by sequential mono-hydroxylations of BbdD. We have previously shown that 2,6-DCBA is hydroxylated by $M6_{bbdD}$ cells yielding 2,6-diCl-3-OHBA [14]. The observed conversion of 2,6-diCl-3-OHBA to 2,6-diCl-3,5-diOHBA and 2,6-diCl-3,4-diOHBA by MSH1 wt cells reported above, suggests a second mono-oxygenation step. However, besides *bbdD* none of the pBAM2 putative catabolic genes encode candidate monooxygenases. Since M6.100g does not convert 2,6-DCBA nor 2,6-diCl-3-OHBA, we hypothesized that BbdD catalyses also the second mono-oxygenation step. To this end, $M6_{bbdD}$ cells were re-examined for the conversion of 2,6-DCBA (with and without NADH added) to test whether, in addition to 2,6-diCl-3-OHBA, also 2,6-diCl-3,5-diOHBA and 2,6-diCl-3,4-diOHBA were produced. In contrast to T'Syen et al. [14], $M6_{bbdD}$ cells were also tested for the conversion of 2,6-diCl-3-OHBA and a crude protein extract of $M6_{bbdD}$ was assayed for conversion of both 2,6-DCBA and 2,6-diCl-3-OHBA. The $M6_{bbdD}$ extract did not convert 2,6-DCBA nor 2,6-diCl-3-OHBA with or without NADH amended. However, $M6_{bbdD}$ cells converted 2,6-DCBA at a rate of 3.54±0.31 E-13 µmol.cell^{-1}.h^{-1}. The presence of NADH did not affect the conversion rate. Apart from 2,6-diCl-3-OHBA, an additional metabolite was detected eluting at the same time in RP-UHPLC as 2,6-diCl-3,5-diOHBA. NMR (Figure S5, Tables S2, S3) spectra were identical to those obtained for 2,6-diCl-3,5-diOHBA (Figure 1, compound A). The same compound was detected when 2,6-diCl-3-OHBA was used as substrate, showing a conversion rate of 4.09±0.18 E-13 µmol.cell^{-1}.h^{-1} which is similar to this of 2,6-DCBA. 2,6-diCl-3,4-diOHBA was neither detected with 2,6-DCBA nor with 2,6-diCl-3-OHBA as substrate. $M6_{pRU}$ did not degrade 2,6-DCBA nor 2,6-diCl-3-OHBA.

2,6-diCl-3,5-diOHBA is dehalogenated into 2-Cl-3,5-diOHBA by the glutathione-dependent dehalogenases BbdI and BbdE. LC-MS/MS and NMR analysis of metabolites produced by MSH1 wt from 2,6-diCl-3-OHBA showed production of 2-Cl-3,5-diOHBA. Therefore, we hypothesized that 2,6-diCl-3,5-diOHBA is converted into 2-Cl-3,5-diOHBA (Figure 1) and that reductive dehalogenation is the next step in the 2,6-DCBA catabolic pathway. BbdI and BbdE both showed amino acid sequence similarity (in the range of 25.6 – 40.3 %) with glutathione-*S*-transferases

(GSTs) involved in dehalogenation of chloroaromatics in other bacterial strains [14]. Crude protein extracts of M6$_{bbdI}$ and M6$_{bbdE}$ indeed converted 2,6-diCl-3,5-diOHBA but only when GSH was present. The rate of 2,6-diCl-3,5-diOHBA conversion by BbdE was approximately 620-fold lower (3.82±0.54 E-03 µmol.mg$_{\text{total protein}}^{-1}$.h^{-1}) than the rate by BbdI (2.38±0.03 µmol.mg$_{\text{total protein}}^{-1}$.h^{-1}), despite similar expression as suggested by the protein intensities in SDS-PAGE (Figure S1). In both cases, 2-Cl-3,5-diOHBA was produced. Both enzymes were also tested towards other pathway intermediates, i.e., 2,6-DCBA, 2,6-diCl-3-OHBA and 2-Cl-3,5-diOHBA, with and without GSH. Only GSH dependent conversion of 2-Cl-3,5-diOHBA was observed but at relatively low rates, i.e., 5.69±1.45 E-03 µmol.mg$_{\text{total protein}}^{-1}$.h^{-1} (BbdI) and 3.66±1.48 E-03 µmol.mg$_{\text{total protein}}^{-1}$.h^{-1} (BbdE). Both enzymes formed 3,5-diOHBA from 2-Cl-3,5-diOHBA by comparison with authentic 3,5-diOHBA in LC-MS/MS. Neither MSH1 wt cells nor protein extracts degraded 3,5-diOHBA, indicating that 3,5-diOHBA is not a pathway intermediate in the degradation of 2,6-DCBA (data not shown).

2-Cl-3,5-diOHBA is hydrolytically dehalogenated by BbdC to 2,3,5-triOHBA. None of the gene functions on pBAM2 could be directly related to degradation of 2-Cl-3,5-diOHBA as the next step in the 2,6-DCBA pathway. However, a crude extract of MSH1 wt did degrade 2-Cl-3,5-diOHBA whereas a crude extract of M6.100g did not (data not shown). From the MSH1 wt crude extract, a highly purified protein fraction showing activity towards 2-Cl-3,5-diOHBA was obtained after AEC and HIC (Figure S6, fraction 5). LC-MS/MS analysis showed that 95.5 % of the protein content of fraction 5 corresponded to the BbdC protein encoded on pBAM2 using the emPAI index approach [19]. The purified protein converted 2-Cl-3,5-diOHBA at a specific rate of 0.277±0.006 µmol.mg$_{\text{BbdC}}^{-1}$.h^{-1}. A crude protein extract of M6$_{bbdC}$ converted 2-Cl-3,5-diOHBA at a conversion rate of 0.330±0.002 µmol.mg$_{\text{total protein}}^{-1}$.h^{-1}, confirming the activity of BbdC towards 2-Cl-3,5-diOHBA (Figure S6). For both the purified protein and the M6$_{bbdC}$ protein extract, a single conversion product (compound D) was detected with RP-UHPLC-MS/MS, which was not further transformed. The [M-H]$^-$ ion of compound D showed a *m/*z of 169.10 and no chlorine isotopic peaks were detected (Table S1) indicating the removal of the residual chlorine. The detected mass (molecular formula $C_7H_6O_5$) suggested that the chlorine was replaced by a hydroxyl group, indicating either hydrolytic or oxygenolytic removal. NMR analysis confirmed these findings

(Figure 2). The ^{1}H NMR spectrum showed resonances of two protons at 6.51 ppm and 6.59 ppm (Figure 2A, Table S2) positioned *meta* to each other (*J* coupling of 2.9 Hz). The ^{13}C NMR spectrum showed seven distinct signals of a main product which indicated that the aromatic moiety is asymmetrically substituted (Figure 2B, Table S3). Based on the ^{1}H-^{13}C HMBC correlation of the proton at 6.59 ppm to the carboxylic group at 172.3 ppm, this proton must be in *ortho* position to the carboxyl group (Figure 2D). All remaining ^{13}C chemical shifts were assigned based on the HSQC and HMBC correlations and compound D was identified as 2,3,5-triOHBA. Confirmation was obtained by comparing LC-MS/MS and NMR results to data obtained from authentic 2,3,5-triOHBA (Figure S4). Activity of the M6$_{bbdC}$ protein extract was also tested towards 2,6-diCl-3-OHBA and 2,6-diCl-3,5-diOHBA. BbdC did not degrade 2,6-diCl-3-OHBA, while 2,6-diCl-3,5-diOHBA was degraded. The conversion rate was 9.27±0.06 E-03 µmol.mg$_{\text{total protein}}^{-1}$.h^{-1}, i.e., 36-fold lower than the rate of 2-Cl-3,5-diOHBA conversion (0.330±0.002 µmol.mg^{-1}.h^{-1}) (Figure S7). However, no reaction product was detected by RP-UHPLC. We therefore conclude that BbdC is mainly responsible for conversion of 2-Cl-3,5-diOHBA to 2,3,5-triOHBA and that 2,3,5-triOHBA is the next intermediate in the 2,6-DCBA catabolic pathway. To examine whether BbdC dehalogenates 2-Cl-3,5-diOHBA hydrolytically or oxygenolytically, conversion of 2-Cl-3,5-diOHBA by the M6$_{bbdC}$ protein extract was tested under anaerobic conditions. M6$_{bbdC}$ converted 2-Cl-3,5-diOHBA at a rate (0.38±0.03 µmol.mg^{-1}.h^{-1}) that was similar to this in the presence of oxygen. 2,3,5-triOHBA was produced concomitantly, providing evidence for a hydrolytic dehalogenation reaction. MSH1 wt did not grow in MS medium containing authentic 2,3,5-triOHBA as the sole C-source. The medium containing high concentrations of 2,3,5-triOHBA rapidly turned brown, likely due to oxidation of the catechol-like 2,3,5-triOHBA.

Aromatic ring cleavage of 2,3,5-triOHBA is catalysed by BbdF. 2,3,5-triOHBA contains vicinal hydroxyl groups (Figure 2) which is a typical configuration for aromatic ring cleavage and is thus a candidate for aromatic ring cleavage [20]. Morever, BbdF shows similarity with type I extradiol dioxygenases such as the catechol 2,3-dioxygenases XylE of *Labrenzia alba* (unreviewed protein sequences, Uniprot, 71.3 % amino acid similarity) and LapB of *Pseudomonas alkylphenolica* (protein data bank proteins, NCBI, 26.76 % amino acid similarity) [14]. Crude protein extracts of M6$_{bbdF}$ indeed converted 2,3,5-triOHBA at a rate of 2.52±0.05 µmol.mg$_{\text{total protein}}^{-1}$.h^{-1}. LC-MS/MS

of the supernatant, analysed immediately after complete substrate conversion, showed that a compound (compound E) was formed with an $[M-H]^-$ ion of *m/z* 201.10 and major fragments at m/z 129.20, 57.15 and 41.15, from which a molecular formula of $C_7H_6O_7$ was deduced. However, upon storage and preparation for NMR analysis, compound E was not detected anymore and instead a compound with an $[M-H]^-$ ion of *m/z* 183.10 (compound F, molecular formula of $C_7H_4O_6$) appeared. The latter compound was identified as chelidonic acid by NMR (Figure S8). GC-MS analysis provided more information about the structure of compound E (Figure 3). Three major peaks were observed. The compounds eluting at 11.8 min and 17.7 min could be identified as the trimethylsilyl (TMS) derivatives of glycerol (present in the lysis buffer of the crude protein extracts) and chelidonic acid, respectively, as their retention times and mass chromatograms were identical to those of the TMS derivatives of the authentic compounds. The compound eluting at 17.3 min was identified as the TMS derivative of 2,4,6-trioxoheptanedioic acid. It showed an electron ionization mass spectrum with major fragment ions that can be interpreted as follows: *m/e* 418, M^+ (0.05%); 403, M^+–15, loss of CH_3; 385, M^+–33, loss of CH_3 and H_2O; 375, M^+–43, loss of CH_3 and CO; 301, M^+–117, loss of $C_4H_9O_2Si$; 259 (base peak); M^+-159, loss of $C_6H_{11}O_3Si$; 147, $C_5H_{15}OSi_2^+$; 73, $C_3H_9Si^+$. The fragmentation pattern of the spectrum (Figure 3E) is in agreement with the mass spectra of the TMS derivatives of similar *meta* cleavage products [21–24]. The loss of CO from the $(M-15)^+$ ion forming *m/e* 375 is characteristic for TMS derivatives of α-hydroxy acids [24] whereas the peak at *m/e* 301 formed by the loss of carboxytrimethylsilyl from the molecular ion is indicative for *meta* cleavage compounds [21–24]. The low abundance (0.05%) of the molecular ion (M^+) and the invariable presence of the $(M-15)^+$ ion, which can be prominent and serves for determining the molecular weight, are typical features of electron ionization mass spectra of TMS derivatives [25].

Glutathione is reduced by $BbdJ_4$. Our results showed that both BbdI and BbdE used GSH to dechlorinate 2,6-diCl-3,5-diOHBA into 2-Cl-3,5-diOHBA. As such, there is a need to replenish GSH. $BbdJ_4$ shows 49.3 % to 65.1 % amino acid similarity with glutathione reductases [14] which reduce GSSG to GSH by oxidizing NADPH to $NADP^+$. A spectrophotometric assay that measures conversion of GSSG into GSH indeed showed that $BbdJ_4$ reduces GSSG when NADPH was present. The GSSG conversion rate was 25.48 µmol. $mg_{total\ protein}^{-1}.h^{-1}$ (Figure S9).

Discussion

Biodegradation of (D)CBAs has been extensively studied in various genera such as *Rhodococcus*, *Alcaligenes*, *Pseudomonas* and *Burkholderia* [26,27]. In general, biodegradation of (D)CBAs follows similar pathways. They are typically dioxygenated and then ring-cleaved. Dechlorination occurs before and/or after ring cleavage and thus the intermediate for ring cleavage is either (chloro)catechol, (chloro)protocatechuate or (chloro)gentisate [27–31]. The only exceptions to this pattern are the hydrolytic dehalogenation pathways of 4-CBA and 2,4-DCBA which do not use hydroxylating dioxygenases [32,33]. The 2,6-DCBA catabolic pathway in MSH1 (Figure 4) shows several deviations from other reported (D)CBA catabolic pathways. As demonstrated by T'Syen *et al.* [14], 2,6-DCBA that is produced from BAM (Figure 4, step I) is first hydroxylated by BbdD to 2,6-diCl-3-OHBA (step II). In this study, we showed that BbdD also performed the second hydroxylation to yield 2,6-diCl-3,5-diOHBA (step III). Only intact cells of MSH1 wt and M6$_{bbdD}$ showed activity towards 2,6-DCBA and 2,6-diCl-3-OHBA. Likely, the extraction step affected BbdD activity by disrupting interactions between the oxygenase and reductase subunits. As reported previously, BbdD shows similarity with oxygenase subunits of Rieske type non-heme iron aromatic ring hydroxylating oxygenases, such as the VanA oxygenase subunit of the VanAB oxidoreductase of *Pseudomonas* sp. HR199 [14]. These enzymes require a reductase subunit that shuffles the electrons from NADH to the oxygenase subunit. For BbdD, the reductase subunit is likely BbdH since BbdH shows similarity with VanB although no evidence was obtained [14]. In M6$_{bbdD}$ cells, related host proteins likely take over the role of BbdH to shuffle electrons to BbdD. Successive hydroxylation of aromatic compounds by the same monooxygenase enzyme complex within a catabolic pathway is not unique but was never reported for (D)CBA catabolism. Toluene catabolism in *Ralstonia pickettii* PKO1 and *Burkholderia cepacia* G4 initiates through two consecutive hydroxylations to produce dihydroxylated aromatics by one mono-oxygenase in both organisms [34,35].

Step IV of the 2,6-DCBA catabolic pathway is thiolytic dehalogenation of 2,6-diCl-3,5-diOHBA into 2-Cl-3,5-diOHBA by the GSTs BbdI and BbdE. Both enzymes showed GSH depended dehalogenation of 2,6-diCl-3,5-diOHBA. However, the activity of BbdE towards 2,6-diCl-3,5-diOHBA was at least 600-fold lower than the activity of BbdI while both proteins were present at

equal amounts in the protein extracts. Whole-cell proteomic analysis of MSH1 wt grown on BAM as sole carbon source suggests that both proteins are equally expressed in MSH1 (Horemans, unpublished results). Therefore, BbdI is likely the main catalyst in 2,6-diCl-3,5-diOHBA conversion in MSH1 unless differences exist in the kinetic properties of the two enzymes. Few GSTs that act as dehalogenases on chlorinated aromatic compounds were reported [36–39], i.e., 3,6-dichlorogentisate dehalogenase DsmH2 involved in the catabolism of dicamba in *Rhizorhabdus dicambivorans* [37], LinD that dechlorinates 2,5-dichlorohydroquinone during the catabolism of lindane in *Sphingomonas paucimobilis* UT26 [38] and tetrachlorohydroquinone (TCHQ) dehalogenase PcpC involved in the degradation of pentachlorophenol in *Sphingobium chlorophenolicum* [39]. BbdE and BbdI are related to PcpC, LinD and DsmH2. These were recently shown to belong to a novel eta class of GSTs that primarily consisted of bacterial GSTs that dehalogenate haloaromatics [37]. Interestingly, DsmH2, LinD and PcpC all require two *para*-substituted hydroxyl groups for dechlorination and are not active on mono-hydroxylated chlorinated aromatics [37]. BbdI and BbdE also seem to require substrates with two hydroxyl groups on opposite sides of the aromatic ring since they did not dehalogenate 2,6-diCl-3-OHBA. However, the BbdI and BbdE substrates contained two *meta*-substituted hydroxyl groups. A thiolytic mechanism for dehalogenation of TCHQ by PcpC has been suggested and BbdE and BbdI likely follow a similar dehalogenation mechanism (Figure S10) [40]. Ketonisation of the aromatic ring results into the formation of 2,6-dichloro-3-hydroxy-5-oxocyclohexa-1,3-diene-1-carboxylic acid. The keto intermediate undergoes a nucleophilic substitution with glutathione thiolate (GS-) that displaces the chlorine atom on the carbon next to the keto group. The thioester bond with GS is then attacked by an active site Cys and 2-Cl-3,5-diOHBA is released, whereas the resulting Cys-glutathione thioester reacts with a second GS- to restore the active site Cys.

Replenishment of GSH is, at least, catalysed by $BbdJ_4$ as it reduces GSSG with the use of NADPH as cofactor (Figure S9). The *bbdJ* gene is present on pBAM2 in conjunction with *bbdI* [14]. Also the gene encoding the related DsmH2 GST is flanked by a gluthatione reductase gene within a larger gene cluster for dicamba degradation in *R. dicambivorans* Ndbn-20 [37]. Moreover, the *bbdI-bbdJ* gene cluster is present on pBAM2 as a four-copy repeat. The four BbdI proteins are 100 % identical. The same counts for the four BbdJ proteins except that $BbdJ_4$ contains an additional 41

amino acid C-terminal stretch of unknown function. Likely, $BbdJ_1$-$BbdJ_3$ are also functional since they contain the active site cysteine residues (Cys^{61}, Cys^{66}) and the FAD- and NADPH-binding domains. The amplification of the *bbdI-bbdJ* gene tandem might indicate that dehalogenation of 2,6-diCl-3,5-diOHBA is a bottleneck in the 2,6-DCBA catabolic pathway and that such increased copy number is required for sufficient activity.

Removal of the residual chlorine of 2-Cl-3,5-diOHBA is achieved by BbdC that replaces the chlorine atom with a hydroxyl group (Step V). We show evidence that BbdC dehalogenates BbdC hydrolytically and not oxygenolytically. Phylogenetic analysis (Figure S11 A) supports this as BbdC is a member of the α/β hydrolase (ABH) superfamily. The ABH superfamily includes type I and type II haloalkane dehalogenases and the fluoroacetate dehalogenases (FAcDHs). BbdC is related to FAcDHs but appears to form a distinct subcluster together with a protein of a metagenomic sequence NORP83 which has 66 % amino acid identity with BbdC [41]. Chan *et al.* [42] developed a decision tree to divide ABH dehalogenases into their subtypes based on the active site residues. BbdC displays deviations from these diagnostic motifs at the active site and cannot be accurately assigned to one of the existing subtypes (Figure S11 B). To the best of our knowledge, BbdC is the first ABH dehalogenase reported to act on an aromatic compound, apparently requiring deviations from the diagnostic motifs of known ABH dehalogenases. We therefore propose BbdC as the prototype of a new subtype of ABH dehalogenases. Only two other hydrolytic dehalogenases that act on aromatic compounds are known [43–45]. The first is 4-chlorobenzoyl-CoA dehalogenase which is involved in 4-chorobenzoate dehalogenation in various bacterial strains such as *Pseudomonas* sp. CBS3, *Arthrobacter* sp. TM1, *Alcaligenes denitrificans* NTB-1 [33,46,47]. 4-chlorobenzoate is first activated by formation of a thioester with CoA by 4-chlorobenzoate-CoA ligase in an ATP dependent reaction. This reaction is a prerequisite for 4-chlorobenzoyl-CoA dehalogenase to replace the chlorine with a hydroxyl group [45]. The second is chlorothalonil hydrolytic dehalogenase, Chd, of *Pseudomonas* sp. CTN-3, which belongs to the metallo-β-lactamases and hydrolytically dehalogenates chlorothalonil [44]. The proposed dehalogenation mechanisms of 4-chlorobenzoyl-CoA dehalogenase and Chd are based on nucleophilic aromatic substitution reactions, which require an electron deficient aromatic moiety and hence electron withdrawing substituents. In case of 4-chlorobenzoyl-CoA, the CoA-thioester bond is the electron

withdrawing substituent while for chlorothalonil, the nitrile groups are electron withdrawing. However, 2-Cl-3,5-diOHBA only contains electron donating groups and the reaction with BbdC was ATP-independent which indicates that dehalogenation of 2-Cl-3,5-diOHBA by BbdC follows another, yet unknown mechanism.

Step VI is catalysed by BbdF. The enzyme used 2,3,5-triOHBA as a substrate to form 2,4,6-trioxoheptanedioic acid. The initial identification of the product of BbdF from 2,3,5-triOHBA was hampered by its abiotic conversion to chelidonic acid (Figure 3). The conversion of 2,4,6-trioxoheptanedioic acid to chelidonic acid is likely due to its existence in solution as an equilibrium mixture of several tautomers and the subsequent transformation reactions shown in Figure S12. Spontaneous conversion of 2,4,6-trioxoheptanedioic acid has also been suggested during chelidonic acid biosynthesis in cultured plant cells [48]. The production of 2,4,6-trioxoheptanedioic acid from 2,3,5-triOHBA thus shows that the conversion of 2,3,5-triOHBA by BbdF involves 1,2-cleavage. 3,4-cleavage of 2,3,5-triOHBA would give 2-(2,3-dioxopropyl)-3-oxobutanedioic acid as a product but the major fragments of *m/e* 259 and *m/e* 301 observed in GC-MS (Figure 3) cannot be formed from 2-(2,3-dioxopropyl)-3-oxobutanedioic. Also, from this cleavage product it is not possible to form the symmetrical chelidonic acid structure that was observed by NMR (Tables S2, S3) and GC-MS. BbdF contains two vicinal oxygen chelate (VOC) domains and thus appears to belong to the Type I extradiol dioxygenases of the VOC superfamily [20]. Other enzymes belonging to the Type I extradiol dioxygenases include catechol 2,3-dioxygenase XylE involved in toluene catabolism in *Pseudomonas putida* mt-2, homoprotocatechuate-2,3-dioxygenase MndD involved in 3,4-dihydroxyphenylacetic acid catabolism in *Arthobacter globiformis* CM-2 and catechol 2,3-dioxygenase LapB involved in the degradation of long-chain alkyl phenols in *Pseudomonas* sp. KL28 [49–51]. They all share a common H-H-E core region at the active site that helps to coordinate the Fe (II) or Mn (II) cofactor [49–51]. This H-H-E core region is also present in BbdF.

The next step (VII) likely involves hydrolysis of 2,4,6-trioxoheptanedioic acid by BbdG into small organic acids that feeds into the Krebs cycle as it demonstrates similarity with fumarylacetoacetate (FAA) hydrolases, showing the typical FAA pfam domain. However, construction of a recombinant version of $M6_{bbdG}$ was unsuccessful. The FAA hydrolase superfamily also includes isomerases like 2-hydroxy-2,4-diene-1,7-dioate isomerase. Therefore, BbdG might

458 also function as an isomerase towards 2,4,6-trioxoheptanedioic acid before actual hydrolysis.
459 Isomerisation of ring cleavage products before hydrolysis was reported before in *Ralstonia* sp. U2
460 [52]. In strain U2, maleylpyruvate is the ring cleavage product of gentisate and a seven-carbon
461 compound similar to 2,4,6-trioxoheptanedioic acid. Maleylpyruvate is isomerised into
462 fumarylpyruvate by maleylpyruvate isomerase and subsequently hydrolysed into pyruvate and
463 fumarate by fumarylpyruvate hydrolase [52]. In case BbdG performs isomerase activity, hydrolysis
464 should involve an enzyme encoded by the chromosome or plasmids other than pBAM1 and
465 pBAM2 since no additional relevant catabolic gene functions than those reported above are
466 available on pBAM1 and pBAM2. Alternatively, BbdG might perform both functions but to the
467 best of our knowledge, such dual functionality is not yet reported.

468 Steps I to VII in Figure 4 represent the productive and major BAM biodegradation pathway in
469 MSH1 which is supported by the observation that most of the metabolites, in case available as
470 authentic compounds, also supported growth of MSH1 wt as sole source of carbon and energy.
471 However, several side reactions were observed. How these side reactions affect BAM conversion
472 *in vivo* is currently unclear as our observations involve primarily *in vitro* expression. One possible
473 *in vivo* side reaction is at the level of BbdD. MSH1 wt cells not only produced 2,6-diCl-3,5-diOHBA
474 but also 2,6-diCl-3,4-diOHBA from 2,6-diCl-3-OHBA. However, the conversion to 2,6-diCl-3,4-
475 diOHBA was not observed with $M6_{bbdD}$ cells., likely due the high expression of BbdD from the
476 strong *bbdA* promotor in $M6_{bbdD}$ compared to its *in vivo* expression. The fate of 2,6-diCl-3,4-
477 diOHBA in MSH1 is currently unclear but the compound appears to be further degraded as its
478 corresponding UHPLC peak ultimately disappeared. Another possible side reaction might be the
479 BbdI/BbdE mediated formation of 3,5-diOHBA from 2-Cl-3,5-diOHBA which is the primary
480 substrate of BbdC. This reaction might be detrimental to strain MSH1 when BbdI and BbdE are
481 expressed *in vivo* at higher levels than BbdC. In that case, BbdI and BbdE will strongly compete
482 with BbdC for dehalogenation of 2-Cl-3,5-diOHBA forming 3,5-diOHBA rather than 2,3,5-triOHBA
483 and hence producing a metabolic dead-end product. However, the *in vitro* activity of BbdC on 2-
484 Cl-3,5-diOHBA was at least 50-fold higher than the activities of BbdI and BbdE while SDS-PAGE
485 analysis indicates similar i*n vitro* expression of recombinant BbdI, BbdE and BbdC. Analysis of the
486 proteome of MSH1 wt grown on BAM revealed that BbdI, BbdE and BbdC are expressed at similar

levels *in vivo* (Horemans, unpublished results). Together these observations indicate that the competition of BbdI and BbdE with BbdC for 2-Cl-3,5-diOHBA under *in vivo* conditions will be limited and hence that 2-Cl-3,5-diOHBA is primarily converted *in vivo* to 2,3,5-triOHBA unless the kinetic parameters of the enzymes show substantial differences. Additionally, MSH1 wt grows on 2-Cl-3,5-diOHBA without production of 3,5-diOHBA and neither 3,5-diOHBA nor 2,3,5-triOHBA are observed when MSH1 wt is grown on BAM as the sole carbon source. More studies aiming at understanding the detailed kinetics and *in vivo* expression of the different enzymes in MSH1 are required to further elucidate the role of the side reactions in BAM catabolism by strain MSH1.

We conclude that 2,6-DCBA, the initial intermediate in the BAM-catabolic pathway of *Aminobacter* sp. MSH1 is further degraded to Krebs cycle intermediates by an unusual catabolic pathway involving steps not reported before in (D)CBA degradation. This new pathway for chloroaromatic catabolism demonstrates the enormous flexibility of bacteria to degrade chlorinated aromatic pollutants. These new insights are important for application of strain MSH1 in DWTPs to treat BAM-contaminated water. For instance, *in situ* monitoring of the pathway intermediates and of the abundances/expression of the catabolic genes will be key for process understanding and control in MSH1 bioaugmented DWTP units.

Figures

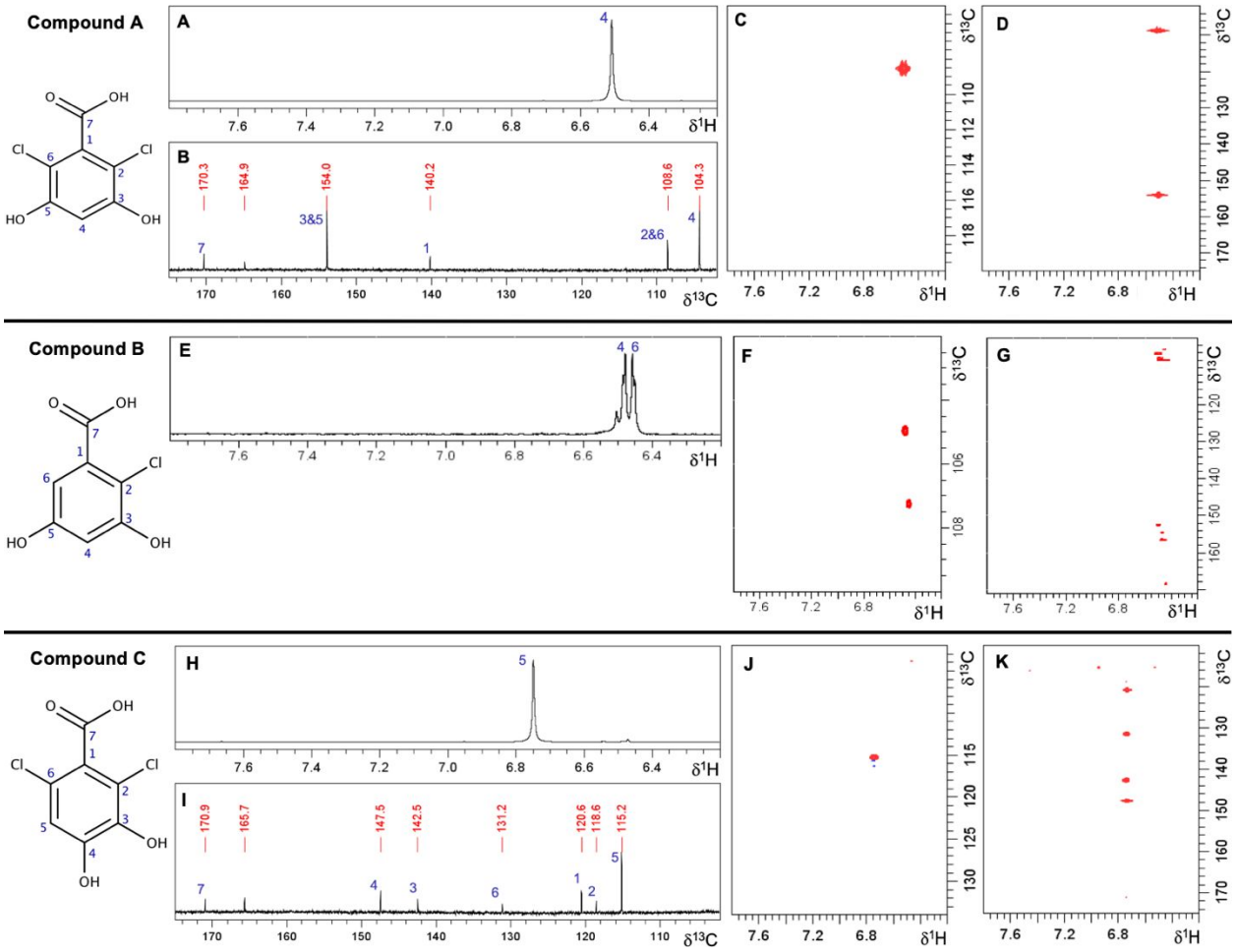

Figure 1. NMR data with signal assignments (in blue) to chemical structures of compounds A (recorded in CD_3OD), B (in DMSO-d_6) and C (in CD_3OD) produced from 2,6-diCl-3-OHBA by MSH1 wt. ^1H NMR spectra are depicted in panels (A), (E) and (H), ^{13}C NMR spectra in (B) and (I), ^1H-^{13}C HSQC spectra in (C), (F) and (J) and ^1H-^{13}C HMBC spectra in (D), (G) and (K). During isolation of compound B, a small amount of compound A was co-purified, explaining the small signal at 6.50 ppm in the ^1H NMR spectrum in panel E and cross peaks at 101.8 ppm, 106.0 ppm and 152.3 ppm in the ^1H-^{13}C HMBC spectrum in panel G.

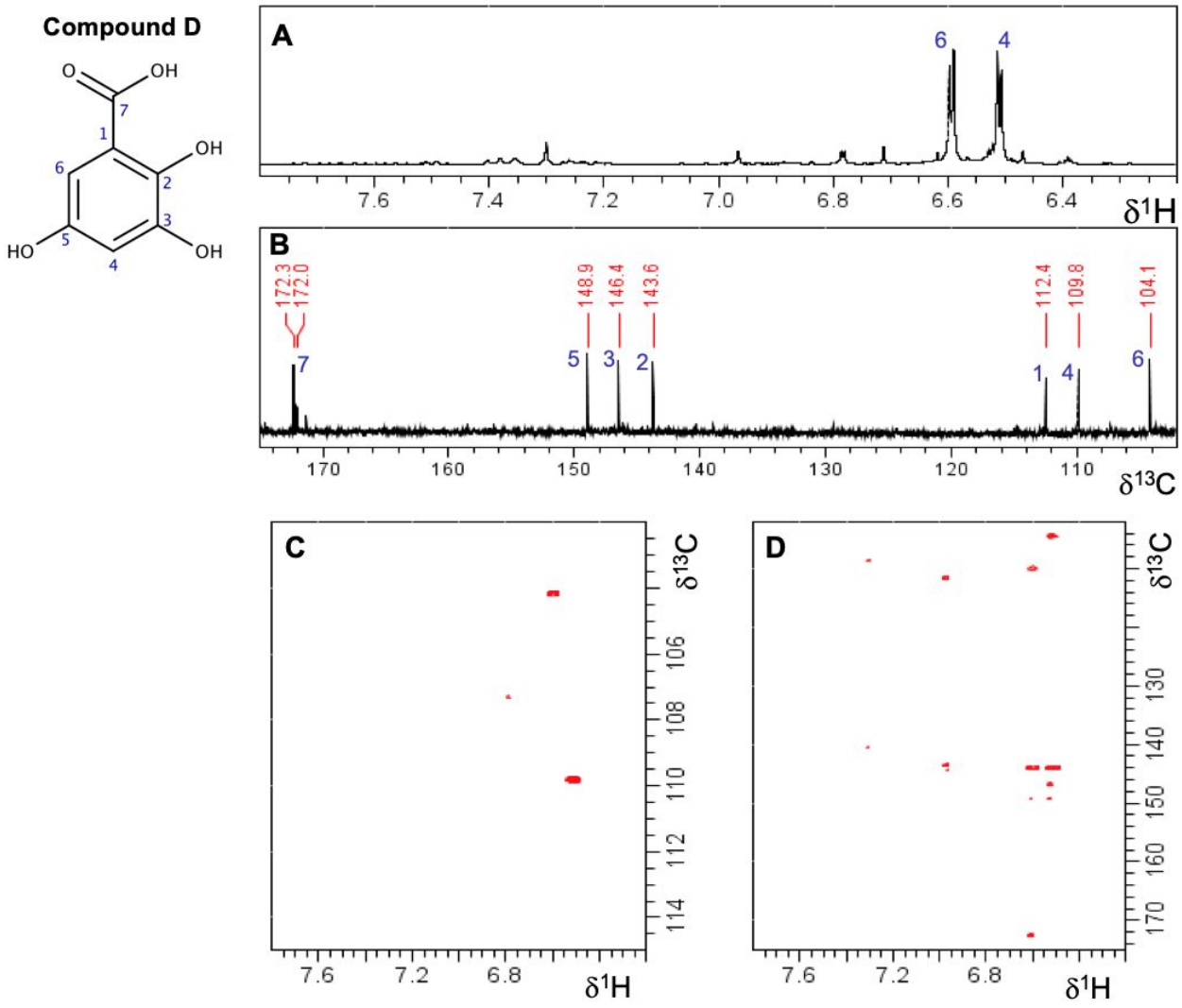

Figure 2. NMR data (recorded in DMSO-d_6) with signal assignment (in blue) of compound D produced by BbdC from 2-Cl-3,5-diOHBA. ^{1}H NMR spectrum in panel (A), ^{13}C NMR spectrum in (B), ^{1}H-^{13}C HSQC spectrum in (C) and ^{1}H-^{13}C HMBC spectrum in (D).

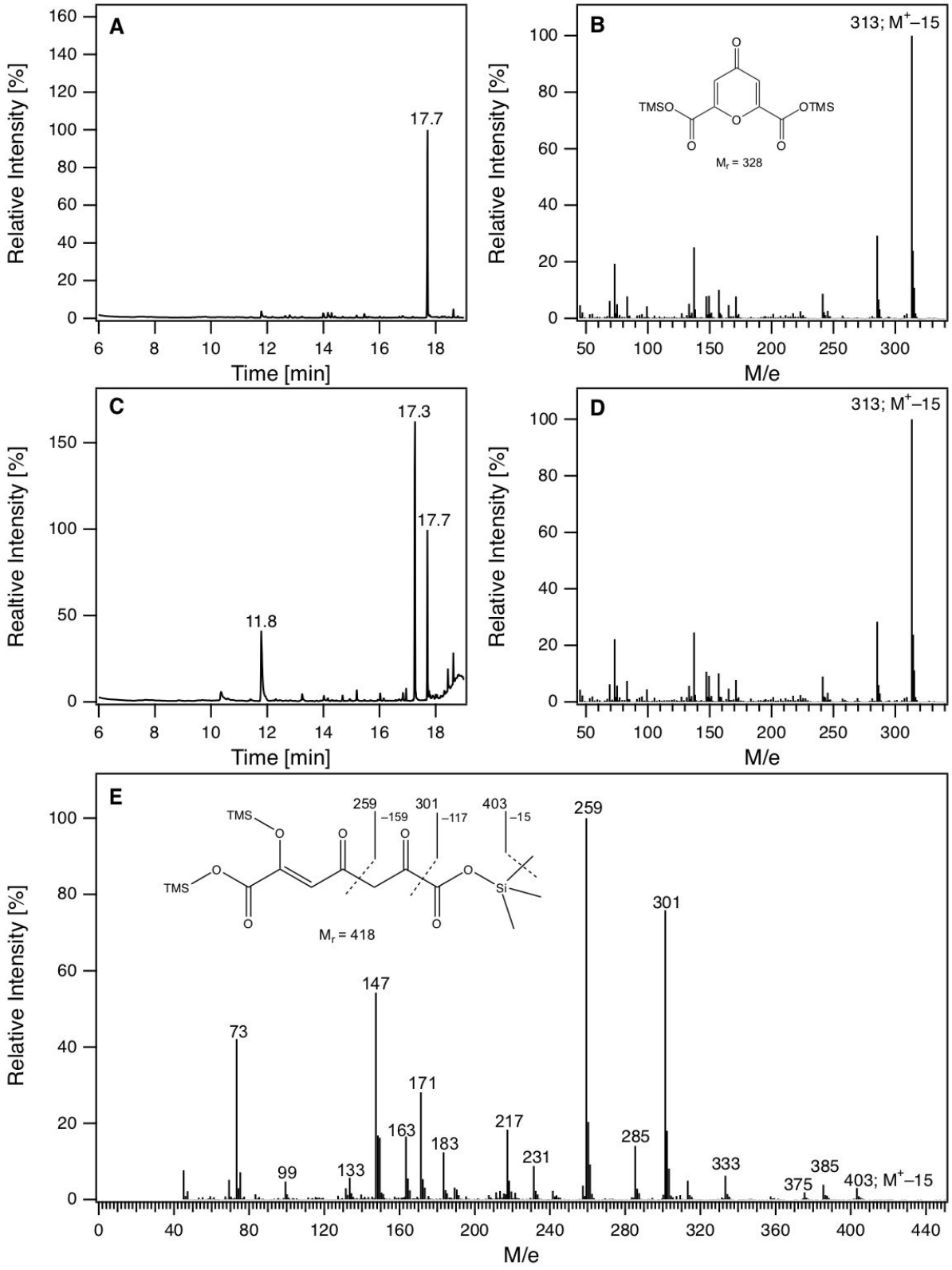
A
Relative Intensity [%]
17.7
Time [min]
B
313; M+–15
TMSO
OTMS
Mr = 328
M/e
C
17.3
17.7
11.8
Realtive Intensity [%]
Time [min]
D
313; M+–15
E
TMS
259
–159
301
–117
403
–15
Mr = 418
73
147
171
163
183
99
133
217
231
259
285
301
333
375
385
403; M+–15
M/e

517

Figure 3. Identification of compounds E and F as 2,4,6-trioxoheptanedioic acid and chelidonic acid respectively, in the supernatant of M6$_{bbdF}$ enzyme assay samples by means of GC-MS. Compounds were extracted with ethyl acetate and derivatized with BSTFA. (A) GC-MS chromatogram of the TMS derivative of authentic chelidonic acid. (B) Electron ionization mass spectrum of the TMS derivative of authentic chelidonic acid. (C) GC-MS chromatogram of the TMS derivatized extract of the M6$_{bbdF}$ enzyme assay sample. Three major peaks can be noted. The compound eluting at 11.8 min was identified as the TMS derivative of glycerol, the compound eluting at 17.7 min was identified as the TMS derivative of chelidonic acid (see panel A, B, and D) and the compound eluting at 17.3 min as the TMS derivative of 2,4,6-trioxoheptanedioic acid (see panel E). (D) Electron ionization mass spectrum of the TMS derivative of the compound eluting at 17.7 min. (E) Electron ionization mass spectrum of the compound eluting at 17.3 min. The insert shows the chemical structure of the compound we inferred from the mass spectrum as well as the fragmentation sites for the major fragments of the mass spectrum.

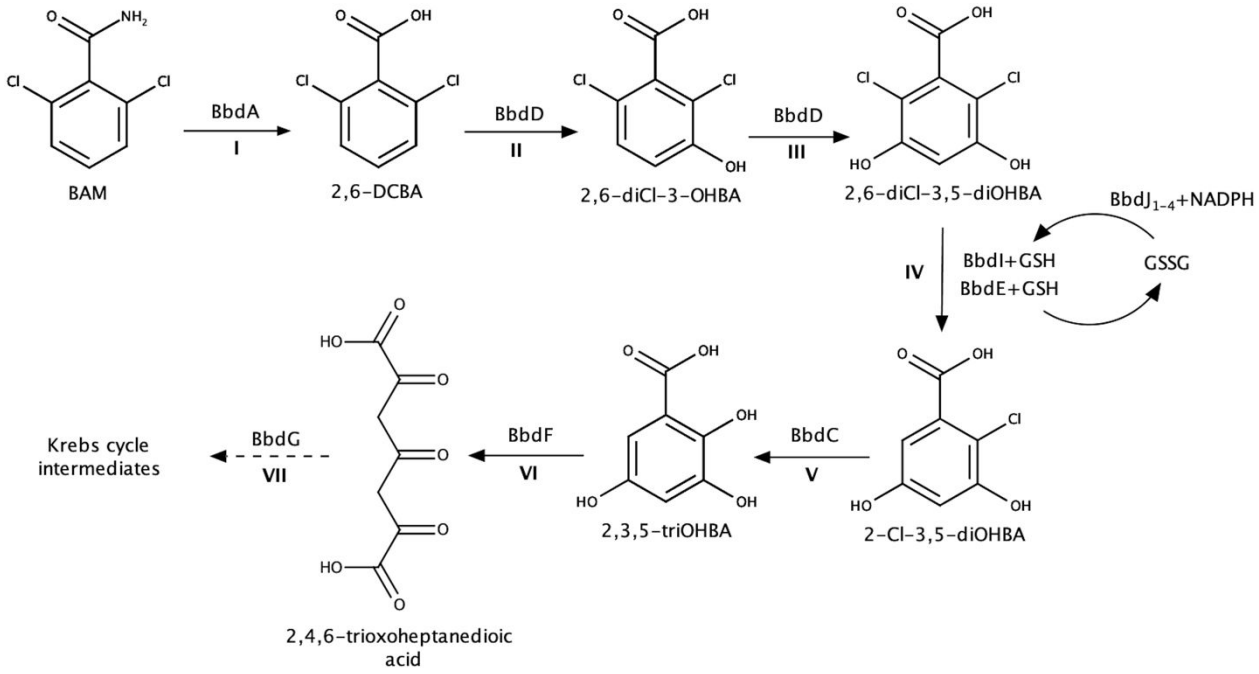

Figure 4. The major BAM catabolic pathway in *Aminobacter* sp. MSH1. BbdA first hydrolyses the amide to the carbonic acid to form 2,6-DCBA (step I) [13]. The BbdD oxygenase then performs a first hydroxylation to yield 2,6-diCl-3-OHBA [14] followed by a second hydroxylation by which 2,6-diCl-3,5-diOHBA is formed (steps II and III). Glutathione-*S*-transferases BbdI and BbdE dechlorinate

2,6-diCl-3,5-diOHBA with use of GSH to form 2-Cl-3,5-diOHBA (step IV). $BbdJ_4$ (and likely $BbdJ_{1-3}$) use NADPH as a cofactor to regenerate GSH from GSSG. 2-Cl-3,5-diOHBA is hydrolytically dechlorinated by BbdC into 2,3,5-triOHBA (step V) which is the substrate for ring cleavage by BbdF yielding 2,4,6-trioxoheptanedioic acid (step VI). BbdG is likely involved in the conversion of 2,4,6-trioxoheptanedioic acid into intermediates of the Krebs Cycle, either by hydrolysing 2,4,6-trioxoheptanedioic acid directly or by isomerisation of 2,4,6-trioxoheptanedioic acid. The isomerisation product is subsequently hydrolysed by a protein encoded by a replicon different from pBAM1 or pBAM2 (step VII). The dashed arrow indicates that the step is not experimentally confirmed. Possible side reactions that were observed in this study, i.e., the production of 2,6-diCl-3,4-diOHBA from 2,6-diCl-3-OHBA by MSH1 wt and the production of the apparent dead-end metabolite 3,5-diOHBA by dechlorination of 2-Cl-3,5-diOHBA by BbdI and BbdE, are not indicated.

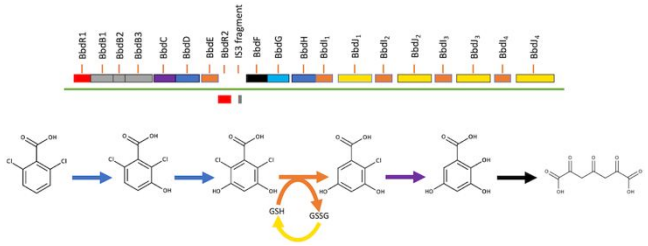

TOC art

Supporting information

Method description for SDS-PAGE (p. S3); SDS-PAGE of crude protein extracts of M6 variants carrying pBAM2 catabolic genes (Fig. S1, p. S3); method description for isolation of BbdC by AEC and HIC p. S4; Description of preparation of pathway intermediates for identification by LC-MS/MS, GC-MS and NMR (p. S5); RP-UHPLC chromatogram of the supernatant of MSH1 wt cells incubated with 2,6-diCl-3-OHBA (Fig S2, p. S7) chemical structures of 2,6-DCBA and pBAM2 pathway intermediates with carbon atom numbers for NMR assignments (Fig. S3, p. 8); NMR data of authentic 2,6-diCl-3,5-diOHBA, 2-Cl-3,5-diOHBA and 2,3,5-triOHBA (Fig. S4, p. 9); NMR data of 2,6-diCl-3,5-diOHBA and 2,6-diCl-3-OHBA produced by $M6_{bbdD}$ cells (Fig. S5, p. S10); SDS-PAGE of collected protein fractions of a crude protein extract of strain MSH1 (Fig. S6, p. S11); Fractions of 2,6-diCl-3-OHBA, 2,6-diCl-3,5-diOHBA and 2-Cl-3,5-diOHBA remaining after incubation with crude

protein extracts of M6$_{bbdC}$ (Fig. S7, p. S11); NMR data of compound F produced by BbdF from 2,3,5-triOHBA and authentic chelidonic acid (Fig. S8, p. S12); Glutathione reducing activity of BbdJ in crude protein extracts of M6$_{bbdJ4}$ (Fig. S9, p. 13); Suggested dehalogenation mechanism of BbdI and BbdE on 2,6-diCl-3,5-diOHBA (Fig. S10, p. 14); Phylogeny of *Aminobacter* sp. MSH1 and related hydrolytic dehalogenases (Fig. S11, p. S15); Putative pathway for the formation of chelidonic acid in incubations of crude extracts of BbdF with 2,3,5-triOHBA (Fig. S12, p. 17); Overview of most abundant *m/z* values of the compounds A, B, C, D and E by means of LC-MS/MS (Table S1, p. 18); ^{1}H NMR chemical shift assignments, coupling constants (*J*) and ^{1}H-^{13}C NMR long range correlations, molecular weights and chemical formulas of detected isolated metabolites and of corresponding authentic compounds (Table S2, p. S20); ^{13}C NMR chemical shift of detected isolated metabolites and authentic compounds (Table S3, p. S22).

Acknowledgements

The authors thank T. Fleischmann and I. Schilling for extensive sample preparation for NMR and GC-MS analysis and D. Grauwels for technical assistance. This work was supported by the KU Leuven C1 project n° C14/15/043 and the BELSPO IAP-project µ-manager n° P7/25. B.H. is supported by the FWO post-doctoral fellow grants 12Q0215N and 12Q0218N. The NMR hardware was partially granted by the Swiss National Science Foundation (SNSF, grant no. 206021_150638/1).

References

(1) Ellegaard-Jensen, L.; Horemans, B.; Raes, B.; Aamand, J.; Hansen, L. H. Groundwater contamination with 2,6-dichlorobenzamide (BAM) and perspectives for its microbial removal. *Appl Microbiol Biotechnol* **2017**, *101* (13), 5235–5245. https://doi.org/10.1007/s00253-017-8362-x.

(2) Törnquist Kreuger, J., Adielsson, S., M. Occurrence of pesticides in Swedish water resources against a background of national risk-reduction programmes — results from 20 years of monitoring. *in: XIII Symposium Pesticide Chemistry — Environmental Fate and Human Health,* **2007**, Piacenza, Italy.

(3) Pukkila, V.; Gustafsson, J.; Tuominen, J.; Aallonen, A.; Kontro, M. H. The most-probable-number enumeration of dichlobenil and 2,6-dichlorobenzamide (BAM) degrading microbes in Finnish aquifers. *Biodegradation* **2009**, *20* (5), 679–686. https://doi.org/10.1007/s10532-009-9255-1.

(4) Porazzi, E.; Martinez, M. P.; Fanelli, R.; Benfenati, E. GC-MS analysis of dichlobenil and its metabolites in groundwater. *Talanta* **2005**, *68* (1), 146–154. https://doi.org/10.1016/j.talanta.2005.04.044.

(5) Herná Ndez-Leal, L.; Temmink, H.; Zeeman, G.; Buisman, C. J. N. Removal of Micropollutants from aerobically treated grey water via ozone and activated carbon. *Water Res.* **2011**, *45*, 2887–2896. https://doi.org/10.1016/j.watres.2011.03.009.

(6) Benner, J.; Helbling, D. E.; Kohler, H. P. E.; Wittebol, J.; Kaiser, E.; Prasse, C.; Ternes, T. A.; Albers, C. N.; Aamand, J.; Horemans, B.; Springael, D. Walravens, E.; Boon, N., Is biological treatment a viable alternative for micropollutant removal in drinking water treatment processes? *Water Res.* **2013**, *47* (16), 5955–5976. https://doi.org/10.1016/j.watres.2013.07.015.

(7) Simonsen, A.; Holtze, M. S.; Sorensen, S. R.; Sorensen, S. J.; Aamand, J. Mineralisation of 2,6-dichlorobenzamide (BAM) in dichlobenil-exposed soils and isolation of a BAM-mineralising *Aminobacter* sp. *Env. Pollut* **2006**, *144* (1), 289–295. https://doi.org/10.1016/j.envpol.2005.11.047.

(8) Holtze, M. S.; Sørensen, S. R.; Sørensen, J.; Hansen, H. C. B.; Aamand, J. Biostimulation and

enrichment of 2,6-dichlorobenzamide-mineralising soil bacterial communities from dichlobenil-exposed soil. *Soil Biol. Biochem.* **2007**, *39* (1), 216–223. https://doi.org/10.1016/j.soilbio.2006.07.009.

(9) Sjøholm, O. R.; Nybroe, O.; Aamand, J.; Sørensen, J. 2,6-dichlorobenzamide (BAM) herbicide mineralisation by *Aminobacter* sp. MSH1 during starvation depends on a subpopulation of intact cells maintaining vital membrane functions. *Environ. Pollut.* **2010**, *158* (12), 3618–3625. https://doi.org/10.1016/j.envpol.2010.08.006.

(10) Sekhar, A.; Horemans, B.; Aamand, J.; Sorensen, S. R.; Vanhaecke, L.; Vanden Bussche, J.; Hofkens, J.; Springael, D. Surface colonization and activity of the 2,6-dichlorobenzamide (BAM) degrading *Aminobacter* sp. strain MSH1 at macro- and micropollutant BAM concentrations. *Environ. Sci. Technol.* **2016**. https://doi.org/10.1021/acs.est.6b01978.

(11) Albers, C. N.; Feld, L.; Ellegaard-Jensen, L.; Aamand, J. Degradation of trace concentrations of the persistent groundwater pollutant 2,6-dichlorobenzamide (BAM) in bioaugmented rapid sand filters. *Water Res.* **2015**, *83*, 61–70. https://doi.org/10.1016/j.watres.2015.06.023.

(12) Horemans, B.; Raes, B.; Vandermaesen, J.; Simanjuntak, Y.; Brocatus, H.; T'Syen, J.; Degryse, J.; Boonen, J.; Wittebol, J.; Lapanje, A.; Sorensen, S. R.; Springael, D. Biocarriers improve bioaugmentation efficiency of a rapid sand filter for the treatment of 2,6-dichlorobenzamide-contaminated drinking water. *Environ. Sci. Technol.* **2017**, *51* (3), 1616–1625. https://doi.org/10.1021/acs.est.6b05027.

(13) T'Syen, J.; Tassoni, R.; Hansen, L. H.; Sorensen, S. J.; Leroy, B.; Sekhar, A.; Wattiez, R.; De Mot, R.; Springael, D. Identification of the amidase BbdA that initiates biodegradation of the groundwater micropollutant 2,6-dichlorobenzamide (BAM) in *Aminobacter* sp. MSH1. *Environ. Sci. Technol.* **2015**. https://doi.org/10.1021/acs.est.5b02309.

(14) T'Syen, J.; Raes, B.; Horemans, B.; Tassoni, R.; Leroy, B.; Lood, C.; van Noort, V.; Lavigne, R.; Wattiez, R.; Kohler, H.-P. E.; Springael, D. Catabolism of the groundwater micropollutant 2,6-dichlorobenzamide beyond 2,6-dichlorobenzoate is plasmid encoded in *Aminobacter* sp. MSH1. *Appl. Microbiol. Biotechnol.* **2018**, *102* (18), 7963–7979. https://doi.org/10.1007/s00253-018-9189-9.

(15) Sørensen, S. R.; Aamand, J. Rapid mineralisation of the herbicide isoproturon in soil from a previously treated Danish agricultural field. *Pest Manag. Sci.* **2003**, *59* (10), 1118–1124. https://doi.org/10.1002/ps.739.

(16) Reasoner, D. J.; Geldreich, E. E. A new medium for the enumeration and subculture of bacteria from potable Water. *Appl. Environ. Microbiol.* **1985**, *49* (1), 1–7.

(17) Breugelmans, P.; Leroy, B.; Bers, K.; Dejonghe, W.; Wattiez, R.; De Mot, R.; Springael, D. Proteomic study of linuron and 3,4-dichloroaniline degradation by *Variovorax* sp. WDL1: evidence for the involvement of an aniline dioxygenase-related multicomponent protein. *Res. Microbiol.* **2010**, *161* (3), 208–218. https://doi.org/10.1016/j.resmic.2010.01.010.

(18) Riddles, P. W.; Blakeley, R. L.; Zerner, B. Ellman's reagent: 5,5'-dithiobis(2-nitrobenzoic acid)--a reexamination. *Anal. Biochem.* **1979**, *94* (1), 75–81.

(19) Ishihama, Y.; Oda, Y.; Tabata, T.; Sato, T.; Nagasu, T.; Rappsilber, J.; Mann, M. Exponentially modified protein abundance index (EmPAI) for estimation of absolute protein amount in proteomics by the number of sequenced peptides per protein. *Mol. Cell. Proteomics* **2005**, *4* (9), 1265–1272. https://doi.org/10.1074/mcp.M500061-MCP200.

(20) Vaillancourt, F.; Bolin, J.; Eltis, L. The ins and outs of ring-cleaving dioxygenases. *Critical Reviews in Biochemistry and Molecular Biology*. **2006**, pp 241–267. https://doi.org/10.1080/10409230600817422.

(21) van der Maarel, M. J. E. C.; Kohler, H.-P. E. Degradation of 2-*sec*-butylphenol: 3-*sec*-butylcatechol, 2-hydroxy-6-oxo-7-methylnona-2,4-dienoic acid, and 2-methylbutyric acid as intermediates. *Biodegradation* **1993**, *4* (2), 81–89. https://doi.org/10.1007/BF00702324.

(22) Kohler, H.-P. E.; Schmid, A.; van der Maarel, M. J. E. C. Metabolism of 2,2'-dihydroxybiphenyl by *Pseudomonas* sp. strain HBP1: production and consumption of 2,2',3-trihydroxybiphenyl. *J. Bacteriol.* **1993**, *175* (6), 1621–1628.

(23) Kohler, H.-P. E.; van der Maarel, M. J. E. C.; Kohler-Staub, D. Selection of *Pseudomonas* sp. strain HBP1 Prp for metabolism of 2-propylphenol and elucidation of the degradative pathway. *Appl. Environ. Microbiol.* **1993**, *59* (3), 860–866.

(24) Massé, R.; Messier, F.; Ayotte, C.; Lévesque, M.-F.; Sylvestre, M. A comprehensive gas

chromatographic/mass spectrometric analysis of 4-chlorobiphenyl bacterial degradation products. *Biol. Mass Spectrom.* **1989**, *18* (1), 27–47. https://doi.org/10.1002/bms.1200180106.

(25) Pierce, A. E. *Silylation of Organic Compounds*; Pierce Chemical Company, **1968**.

(26) Field, J. A.; Sierra-Alvarez, R. Microbial transformation of chlorinated benzoates. *Rev. Environ. Sci. Bio/Technology* **2008**, *7* (3), 191–210. https://doi.org/10.1007/s11157-008-9133-z.

(27) Pieper, D. H. Aerobic degradation of polychlorinated biphenyls. *Appl. Microbiol. Biotechnol.* **2005**, *67* (2), 170–191. https://doi.org/10.1007/s00253-004-1810-4.

(28) Ajithkumar, P. V; Kunhi, A. A. Pathways for 3-chloro- and 4-chlorobenzoate degradation in Pseudomonas *aeruginosa* 3mT. *Biodegradation* **2000**, *11* (4), 247–261. https://doi.org/10.1023/A:1011124220003.

(29) Krooneman, J.; Wieringa, E. B. A.; Moore, E. R. B.; Gerritse, J.; Prins, R. A.; Gottschal, J. C. Isolation of *Alcaligenes* sp. strain L6 at low oxygen concentrations and degradation of 3-chlorobenzoate via a pathway not involving (chloro)catechols. *Appl. Environ. Microbiol.* **1996**, *62* (7), 2427–2434.

(30) Miyashita, K.; Ogawa, N.; Francisco, P. B.; Suzuki, K. The chlorobenzoate dioxygenase Genes of *Burkholderia* sp. strain NK8 involved in the catabolism of chlorobenzoates. *Microbiology* **2015**, *147* (1), 121–133. https://doi.org/10.1099/00221287-147-1-121.

(31) Nakatsu, C. H.; Wyndham, R. C. Cloning and expression of the transposable chlorobenzoate-3,4-dioxygenase genes of *Alcaligenes* sp. Strain BR60. *Appl. Environ. Microbiol.* **1993**, *59* (11), 3625–3633.

(32) Romanov, V.; Hausinger, R. P. NADPH-dependent reductive *ortho* dehalogenation of 2,4-dichlorobenzoic acid in *Corynebacterium sepedonicum* KZ-4 and *Coryneform* bacterium strain NTB-1 via 2,4-dichlorobenzoyl coenzyme A. *J. Bacteriol.* **1996**, *178* (9), 2656–2661. https://doi.org/10.1128/jb.178.9.2656-2661.1996.

(33) Dunaway-Mariano, D.; Babbitt, P. C. On the origins and functions of the enzymes of the 4-chlorobenzoate to 4-hydroxybenzoate converting pathway. *Biodegradation* **1994**, *5* (3–4), 259–276. https://doi.org/10.1007/BF00696464.

695 (34) Fishman, A.; Tao, Y.; Wood, T. K. Physiological relevance of successive hydroxylations of
696 toluene by toluene *para*-monooxygenase of *Ralstonia pickettii* PKO1. *Biocatal.*
697 *Biotransformation* **2004**, *22* (4), 283–289. https://doi.org/10.1080/10242420400012008.
698 (35) Newman, L. M.; Wackett, L. P. Purification and characterization of toluene 2-
699 monooxygenase from *Burkholderia* cepacia G4. *Biochemistry* **1995**, *34* (43), 14066–14076.
700 https://doi.org/10.1021/bi00043a012.
701 (36) Allocati, N.; Federici, L.; Masulli, M.; Di Ilio, C. Glutathione transferases in bacteria. *FEBS J.*
702 **2009**, *276* (1), 58–75. https://doi.org/10.1111/j.1742-4658.2008.06743.x.
703 (37) Li, N.; Tong, R.-L.; Yao, L.; Chen, Q.; Yan, X.; Ding, D.-R.; Qiu, J.-G.; He, J.; Jiang, J.-D. Roles
704 of two glutathione-dependent 3,6-dichlorogentisate dehalogenases in *Rhizorhabdus*
705 *dicambivorans* Ndbn-20 in the catabolism of the herbicide dicamba. *Appl. Environ.*
706 *Microbiol.* **2018**, *84* (17). https://doi.org/10.1128/AEM.00623-18.
707 (38) Miyauchi, K.; Suh, S.-K.; Nagata, Y.; Takagi, M. Cloning and sequencing of a 2,5-
708 dichlorohydroquinone reductive dehalogenase gene whose product is involved in
709 degradation of γ-Hexachlorocyclohexane by *Sphingomonas paucimobilis*. *J. Bacteriol.* **1998**,
710 *180* (6), 1354 LP – 1359.
711 (39) Cai, M.; Xun, L. Organization and regulation of pentachlorophenol-degrading genes in
712 *Sphingobium chlorophenolicum* ATCC 39723. *J. Bacteriol.* **2002**, *184* (17), 4672 LP – 4680.
713 (40) Warner, J. R.; Copley, S. D. Pre-steady-state kinetic studies of the reductive dehalogenation
714 catalyzed by tetrachlorohydroquinone dehalogenase. *Biochemistry* **2007**, *46* (45), 13211–
715 13222. https://doi.org/10.1021/bi701069n.
716 (41) Tully, B. J.; Wheat, C. G.; Glazer, B. T.; Huber, J. A. A dynamic microbial community with
717 high functional redundancy inhabits the cold, oxic subseafloor aquifer. *ISME J.* **2018**, *12* (1),
718 1–16. https://doi.org/10.1038/ismej.2017.187.
719 (42) Chan, W. Y.; Wong, M.; Guthrie, J.; Savchenko, A. V.; Yakunin, A. F.; Pai, E. F.; Edwards, E.
720 A. Sequence- and activity-based screening of microbial genomes for novel dehalogenases.
721 *Microb. Biotechnol.* **2010**, *3* (1), 107–120. https://doi.org/10.1111/j.1751-
722 7915.2009.00155.x.
723 (43) Arora, P. K.; Bae, H. Role of dehalogenases in aerobic bacterial degradation of chlorinated

724 aromatic compounds. *J. Chem.* **2014**, *2014*, 1–10. https://doi.org/10.1155/2014/157974.
725 (44) Wang, G.; Li, R.; Li, S.; Jiang, J. A novel hydrolytic dehalogenase for the chlorinated aromatic
726 compound chlorothalonil. *J. Bacteriol.* **2010**, *192* (11), 2737–2745.
727 https://doi.org/10.1128/JB.01547-09.
728 (45) Scholten, J. D.; Chang, K. H.; Babbitt, P. C.; Charest, H.; Sylvestre, M.; Dunawaymariano, D.
729 Novel enzymatic hydrolytic dehalogenation of a chlorinated aromatic. *Science (80-.).* **1991**,
730 *253* (5016), 182–185. https://doi.org/10.1126/science.1853203.
731 (46) Marks, T. S.; Smith, A. R. W.; Quirk, A. V. Degradation of 4-chlorobenzoic acid by
732 *Arthrobacter* sp. *Appl. Environ. Microbiol.* **1984**, *48* (5), 1020–1025.
733 (47) Van Den Tweel, W. J. J.; Kok, J. B.; De Bont, J. A. M. Reductive dechlorination of 2,4-
734 dichlorobenzoate to 4-chlorobenzoate and hydrolytic dehalogenation of 4-chloro-, 4-
735 bromo-, and 4-iodobenzoate by *Alcaligenes* denitrificans NTB-1. *Appl. Environ. Microbiol.*
736 **1987**, *53* (4), 810–815.
737 (48) Shen, Z.-W.; Fisinger, U.; Poulev, A.; Eisenreich, W.; Werner, I.; Pleiner, E.; Bacher, A.; Zenk,
738 M. H. Tracer studies with 13C-labeled carbohydrates in cultured plant cells.
739 retrobiosynthetic analysis of chelidonic acid biosynthesis. *Phytochemistry* **2001**, *57* (1), 33–
740 42. https://doi.org/10.1016/S0031-9422(00)00496-9.
741 (49) Kita, A.; Kita, S.; Fujisawa, I.; Inaka, K.; Ishida, T.; Horiike, K.; Nozaki, M.; Miki, K. An
742 archetypical extradiol-cleaving catecholic dioxygenase: the crystal structure of catechol
743 2,3-dioxygenase (metapyrocatechase) from *Pseudomonas* putida Mt-2. *Structure* **1999**, *7*
744 (1), 25–34. https://doi.org/10.1016/S0969-2126(99)80006-9.
745 (50) Cho, J.-H.; Jung, D.-K.; Lee, K.; Rhee, S. Crystal structure and functional analysis of the
746 extradiol dioxygenase LapB from a long-chain alkylphenol degradation pathway in
747 *Pseudomonas*. *J. Biol. Chem.* **2009**, *284* (49), 34321–34330.
748 https://doi.org/10.1074/jbc.M109.031054.
749 (51) Que, L.; Wagner, M. L.; Boldt, Y. R.; Wackett, L. P.; Whiting, A. K.; Sadowsky, M. J.
750 Manganese(II) active site mutants of 3,4-dihydroxyphenylacetate 2,3-dioxygenase from
751 *Arthrobacter globiformis* strain CM-2 †. *Biochemistry* **2002**, *36* (8), 2147–2153.
752 https://doi.org/10.1021/bi962362i.

(52) Zhou, N. Y.; Fuenmayor, S. L.; Williams, P. A. Nag genes of *Ralstonia* (formerly *Pseudomonas*) sp. strain U2 encoding enzymes for gentisate catabolism. *J. Bacteriol.* **2001**, *183* (2), 700–708. https://doi.org/10.1128/JB.183.2.700-708.2001.